temperature and was stirred for 1 day. Pumping off the volatile compound left the residual product of which ^{19}F NMR analysis showed 35% yield of adduct **3a** and **4a** (conversion yield is 77%) and starting material. Separation using column chromatography (silica gel, CH_2Cl_2) gave 100 mg of adduct **3a** and **4a** (20%). Purification was completed by recrystallization from pentane. Adduct **3a** and **4a**: mp 81–82 °C; R_f 0.32 (silica gel, CH_2Cl_2); infrared spectrum (KBr) 3530 (m), 3395 (m), 1600 (w), 1505 (s), 1443 (m), 1400 (w), 1285 (vs), 1270 (s), 1230 (vs), 1215 (vs), 1175 (m), 1165 (m), 1120 (m), 1090 (vw), 970 (m), 940 (w), 885 (w), 863 (vw), 848 (vw), 815 (vw), 760 (vw), 720 (w), 660 (vw), 587 (vw), 500 (vw), 410 (vw) cm^{-1}; mass spectrum (*m/e*) M^+ 345, 343, $[(CF_3)_2C{=}S]^+$ 182, $[M - C_3F_7]^+$ 176, 174, $[M - C_3F_7H_2]^+$ 174, 172, $[CF_3CFS]^+$ 132, $[CF_3CS]^+$ 113, $[CF_3]^+$ 69; ^{19}F NMR ($CDCl_3$) ϕ −74.6 (6 F, 2 d, both J = 10.8 Hz), −166.0 (1 F, 2 sept, both J = 10.8 Hz); ^1H NMR ($CDCl_3$) δ 7.4–6.7 (arom), 5.4 (br s), 5.0 (br s); UV (hexane) λ 292 nm (log ϵ = 3.67), 239 (log ϵ = 4.12).

Anal. Calcd for $C_9H_5NF_7ClOS$: C, 31.46; H, 1.47; N, 4.08. Found: C, 31.18; H, 1.48; N, 4.04.

Reaction of Thioxazole 1 with Hydrogen Bromide. To a 100-mL Pyrex glass vessel equipped with a Teflon stopcock and containing thioxazole **1** (300 mg, 0.98 mmol) and diethyl ether (2 mL) was added hydrogen bromide (6.86 mmol) at −196 °C. This mixture was stirred −78 °C for 1 h. After the volatile compound was pumped off, the precipitated ammonium salt was filtered off by using methylene chloride. The filtrate was evaporated to leave crude adduct **3b** and **4b**. This was purified by column chromatography (silica gel, CH_2Cl_2) to give 130 mg of adduct **3b** and **4b** (34%). Recrystallization from pentane afforded the pure adduct **3b** and **4b**: mp 94.5–96.5 °C; R_f 0.19 (silica gel, CH_2Cl_2); infrared spectrum (KBr) 3503 (m), 3383 (s), 1595 (m), 1496 (s), 1440 (s), 1395 (w), 1303 (vs), 1285 (vs), 1265 (vs), 1220 (vs), 1165 (s), 1118 (s), 1080 (vw), 970 (s), 938 (m), 868 (m), 847 (w), 815 (m), 761 (w), 723 (m), 642 (w), 583 (w), , 550 (vw), 410 (w), 385 (vw), 360 (vw) cm^{-1}; mass spectrum (*m/e*) M^+ 389, 387, $[M - CF_4H_2O]^+$, 283, 281, $[M - C_3F_7]^+$ 220, 218, $[M - H_2C_3F_7]^+$ 218, 216, $[C_6H_4SBr]^+$ 189, 187, $[C_6H_3SBr]^+$ 188, 186, $[(CF_3)_2CS]^+$ 182, $[CF_2(CF_3)CS]^+$ 163, $[CFSOBr]^+$ 160, 158, $[CFS(NH)Br]^+$ 159, 157, $[CF_3(F)CS]^+$ 132, $[CF_3CS]^+$ 113, $[CF_2CS]^+$ 94, $[CF_3]^+$ 69; ^{19}F NMR ($CDCl_3$) ϕ −74.5 (6 F, 2 d, both J = 10.7 Hz), −165.5 (1 F, 2 sept, both J = 13.3 Hz); ^1H NMR ($CDCl_3$) δ 7.6–6.9 (arom), 5.4 (br s).

Anal. Calcd for $C_9H_5NF_7BrOS$: C, 27.86, H, 1.30. Found: C, 28.04; H, 1.43.

Acknowledgment is expressed to the donors of the Petroleum Research Fund, administered by the American Chemical Society, and to the National Science Foundation (Grant CHE-7727395) for support of this research. We thank Charles Barinaga and Dennis Gage for mass and ^{19}F NMR spectral data.

(η^2-Olefin)tetracarbonylruthenium Complexes: Photochemical Syntheses from Dodecacarbonyltriruthenium and Quantum Yield Determinations

Friedrich-Wilhelm Grevels,*[1] Johannes G. A. Reuvers,*[1] and Josef Takats*[1]

Contribution from the Institut für Strahlenchemie im Max-Planck-Institut für Kohlenforschung, D-4330 Mülheim a.d. Ruhr, Federal Republic of Germany. *Received August 27, 1980*

Abstract: Photolysis of dodecacarbonyltriruthenium in the presence of excess olefin (methyl acrylate, dimethyl fumarate, dimethyl maleate, allyl acrylate, methyl vinyl ketone, and acrylonitrile) results in quantitative formation of (η^2-olefin)tetracarbonylruthenium complexes, some of which are isolated as white crystalline solids. Disappearance quantum yields, $\phi_{-Ru_3(CO)_{12}}$, are in the range of 0.003–0.12, depending on the olefin (methyl acrylate to dimethyl fumarate), its concentration, and the incident wavelength (λ = 313 and 395 nm). Mechanistic aspects are discussed. The infrared and NMR spectroscopic data of the (η^2-olefin)$Ru(CO)_4$ complexes indicate that the metal → π^*(olefin) interaction is strengthened in comparison with the analogous iron compounds, while the metal → π^*(CO) back-donation is decreased. Due to its moderate stability, (η^2-methyl acrylate)$Ru(CO)_4$ may be used as a source of $Ru(CO)_4$ thus providing another route to L-$Ru(CO)_4$ complexes.

In contrast to the various synthetic routes known for the complexes (η^2-olefin)$Fe(CO)_4$[2] no general high-yield synthesis of the analogous ruthenium compounds has been reported. (Ethylene)$Ru(CO)_4$[3] and (1-pentene)$Ru(CO)_4$[4] were generated by photolysis of $Ru_3(CO)_{12}$ in the presence of excess olefin and identified in situ by their infrared spectra. Recently, the quantum yield of such reactions was mentioned to be $\phi \approx 10^{-2}$, but no account was given of the actual isolation and characterization of these compounds.[4,5] (η^2-Olefin)$Ru(CO)_4$ complexes of ethyl acrylate and diethyl fumarate were prepared analogously and characterized by infrared and variable-temperature ^{13}C NMR spectroscopy and mass spectrometry;[6] however, it proved to be difficult to obtain analytically pure materials.

Scheme I

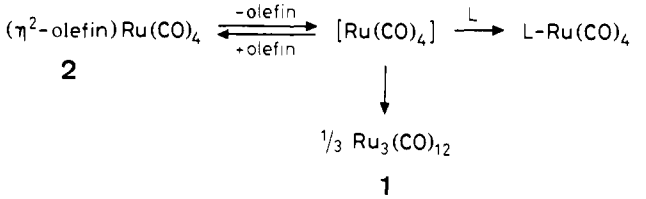

In this contribution we describe a convenient procedure for the photochemical preparation of (η^2-olefin)$Ru(CO)_4$ complexes from $Ru_3(CO)_{12}$. Quantum yields have been determined under various

(1) Address correspondence to any of the authors.
(2) King, R. B. In "The Organic Chemistry of Iron"; Koerner von Gustorf, E. A., Grevels, F.-W., Fischler, I., Eds.; Academic Press: New York, 1978; Vol. I, p 397.
(3) Johnson, B. F. G.; Lewis, J.; Twigg, M. V. *J. Organomet. Chem.* **1974**, *67*, C75.
(4) Austin, R. G.; Paonessa, R. S.; Giordano, P. J.; Wrighton, M. S. *Adv. Chem. Ser.* **1978**, *No. 168*, 189.
(5) Graff, J. L.; Sanner, R. D.; Wrighton, M. S. *J. Am. Chem. Soc.* **1979**, *101*, 273.
(6) Kruczynski, L.; Martin, J. L.; Takats, J. *J. Organomet. Chem.* **1974**, *80*, C9.

0002-7863/81/1503-4069$01.25/0

Table I. ν(CO) Infrared Data (cm^{-1}) of the (η^2-Olefin)$Ru(CO)_4$ Complexes **2**[a]

complex	olefin	carbonyl ligands $A_1^{(1)}$	B_1[b]	$A_1^{(2)}$	B_2	ester carbonyl groups
2a[c,e]	methyl acrylate	2121 (0.16)	2049.5 (1.30)	2035 (1.19)	2008.5 (1.35)	1715
2b[c]	dimethyl fumarate	2133 (0.20)	2066[f] (1.73)	2051.5 (0.60)	2019 (1.47)	1730 (w), 1718 (sh), 1713
2c[c]	dimethyl maleate	2133[g] (0.23)	2065[h] (1.33)	2040.5 (1.06)	2018.5 (1.38)	1748 (sh), 1736, 1731 (sh), 1717
2d[d,e]	allyl acrylate[i]	2124	2052	2037	2011	1711
2e[d,e]	methyl vinyl ketone	2123	2050	2038	2007	1681
2f[d,e]	acrylonitrile	2125	2055.5	2044.5	2021	
2g[d,e]	1-pentene	2103	2021[k]		1994	
2h[d,s]	maleic anhydride	2146	2078	2072	2047	1823, 1759

[a] In hexane at ambient temperature. [b] ν_{as} of the axial CO ligands. [c] Recorded on Perkin-Elmer 580 instrument, calibrated with DCl,[31] relative integrated intensities in parentheses. [d] Recorded on Perkin-Elmer 257 instrument. [e] Recorded in the presence of excess olefin. [f] Weak shoulder at ~2063 cm^{-1}. [g] Weak shoulder at ~2128 cm^{-1}. [h] Shoulder at ~2061 cm^{-1}. [i] One isomer only, apparently exclusive coordination via the acrylate rather than the allylic C=C moiety; [k] overlapping bands.

conditions and will be discussed under mechanistic aspects.

Results and Discussion

Synthesis of (η^2-Olefin)$Ru(CO)_4$ Complexes. Upon irradiation in the presence of excess olefin in hexane solution, $Ru_3(CO)_{12}$ (**1**)

$$\underset{\mathbf{1}}{Ru_3(CO)_{12}} + 3\text{olefin} \xrightarrow[T \lesssim 15\ ^\circ C]{h\nu,\ \lambda \gtrsim 370\ nm} 3\underset{\mathbf{2}}{(\eta^2\text{-olefin})Ru(CO)_4} \quad (1)$$

is quantitatively converted into the respective (η^2-olefin)$Ru(CO)_4$ complexes **2** (see Table I), some of which are stable enough to be isolated as analytically pure, white crystalline solids. The products are screened from further irradiation by a cutoff filter ($\lambda \gtrsim 370$ nm) which impedes secondary photoreactions such as formation of the (surprisingly stable) (η^2-olefin)$_2Ru(CO)_3$ complexes[7] but is transparent in the region of the long wavelength absorption maximum of the starting material **1** at 390 nm.

The fumarate and maleate derivatives **2b** and **2c** are fairly stable at room temperature. **2a** is less stable, and solutions of, e.g., **2d–2f** readily decompose with formation of $Ru_3(CO)_{12}$. **2e** and **2g** (cf. ref 4) have not been isolated but were generated and characterized in situ by their infrared spectra (cf. Table I). Apparently, an equilibrium is established involving the uncoordinated olefin and the species [$Ru(CO)_4$] which finally leads to the trinuclear cluster **1** (Scheme I). Excess free olefin shifts the equilibrium toward the left, thus preventing the decomposition of complexes **2** and facilitating the workup of the reaction mixtures. Isolated complexes can be stored indefinitely as solids under an argon atmosphere at appropriate low temperatures.

The moderate stability of **2a** at room temperature establishes it as a potentially useful source of the species [$Ru(CO)_4$], thus providing another route to a variety of L–$Ru(CO)_4$ complexes via ligand exchange (cf. Scheme I) with, e.g., L = maleic anhydride, trimethyl phosphite, or triphenylphosphine.[8] **2a** also reacts with dienes to yield several products among which are (η^4-diene)$Ru(CO)_3$ complexes.[8] Upon treatment with carbon monoxide at ambient temperature in the dark, **2a** is slowly converted into $Ru(CO)_5$; some decomposition to $Ru_3(CO)_{12}$ also occurs. These reactions are suppressed in the presence of excess methyl acrylate.

Conversion of $Ru_3(CO)_{12}$ into complex **2g** (cf. ref 4) is not complete, even after prolonged irradiation in the presence of a large excess of 1-pentene. Apparently, a photostationary state is reached, and upon switching off the light source, we observed reformation of $Ru_3(CO)_{12}$.

Under an atmosphere of carbon monoxide the irradiation of $Ru_3(CO)_{12}$, even in the presence of a 30-fold excess of methyl acrylate, leads to the formation of both $Ru(CO)_5$ and (η^2-methyl acrylate)$Ru(CO)_4$ (**2a**) at the early stages of the reaction. Prolonged irradiation yields **2a** as the sole final product which is stable under these conditions. Apparently, the excess of methyl acrylate is sufficient to preclude the reaction of **2a** with carbon monoxide.

Physical Properties of (η^2-Olefin)$Ru(CO)_4$ Complexes. The infrared spectra of the complexes **2** (Table I, Figure 1) exhibit four bands in the metal carbonyl region (two of which are overlapping in the case of **2g**), consistent with the expected trigonal-bipyramidal geometry in which the olefin occupies an equatorial position (C_{2v} local symmetry with four infrared active ($2A_1$, B_1, B_2) CO stretching vibrations[9]). The spectra of **2a–2c** are analyzed by using Bor's method[10] which has been adapted to $M(CO)_4$ C_{2v} local symmetry.[11] The bands of **2b** are assigned to the $A_1^{(1)}$ [ν_s(ax-CO)], $A_1^{(2)}$ [ν_s(eq-CO)], B_2 [ν_{as}(eq-CO)], and B_1 [ν_{as}(ax-CO)] CO stretching vibrations in the order of increasing

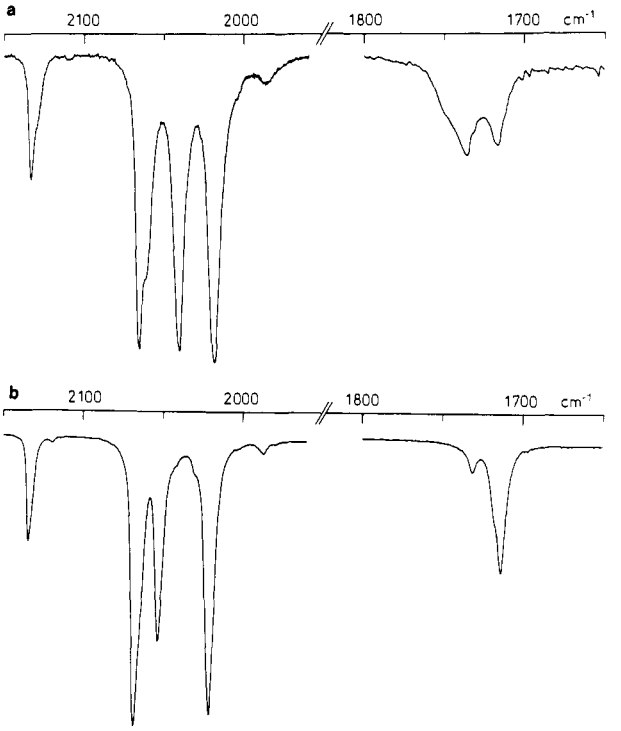

Figure 1. ν(CO) regions in the infrared spectra of (a) (η^2-dimethyl maleate)$Ru(CO)_4$ (**2c**) and (b) (η^2-dimethyl fumarate)$Ru(CO)_4$ (**2b**).

Table II. ν(CO) Force Field Parameters for (η^2-Olefin)$M(CO)_4$ Complexes

	M	olefin	k and i, mdyn $Å^{-1}$ k_a	k_e	i_a	i_e	i_{ea}
2a	Ru	methyl acrylate	17.49	16.60	0.52	0.30	0.23
2b	Ru	dimethyl fumarate	17.64	16.91	0.39	0.44	0.30
2c	Ru	dimethyl maleate	17.67	16.78	0.44	0.32	0.30
	Fe	dimethyl fumarate[11]	17.19	16.81	0.26	0.55	0.29

(7) Grevels, F.-W.; Reuvers, J. G. A.; Takats, J. *Angew. Chem.*, in press.
(8) Grevels, F.-W.; Reuvers, J. G. A., unpublished results.
(9) Braterman, P. S. In "Metal Carbonyl Spectra"; Academic Press: London, 1975.
(10) Bor, G. *Inorg. Chim. Acta* **1967**, *1*, 81.
(11) Grevels, F.-W.; Koerner von Gustorf, E. *Justus Liebigs Ann. Chem.* **1973**, 1821.

Table III. ^{13}C NMR Spectroscopic Data of (η^2-Olefin)M(CO)$_4$ Complexes[a]

	olefin	M	δ[b] C(1)	C(1′)	C(2)	C(3)	CO	$\Delta\delta$[c] C(1)	C(1′)	C(3)
2a	$^{(1')}CH_2$ ‖ $^{(1)}CH-CO_2CH_3$ $^{(3)}\ ^{(2)}$	Ru	35.5[d] (d, 159)	23.9 (t, 161)	51.1 (q, 148)	176.3	193.6, 194.8, 195.5, 197.6[e]	93.4	106.4	−10.1
		Fe	44.2 (d, 166)	34.3 (t, 164)	51.2 (q. 147)	174.6	208.6	84.7	96.0	−8.4
2b	$^{(1)}\ ^{(3)}\ ^{(2)}$ $HC-CO_2CH_3$ ‖ CH_3O_2C-CH	Ru[f]	37.1 (d, 164)		51.3 (q, 146)	175.7	190.6, 193.6	96.2		−10.8
		Fe	44.5 (d, 164)		51.5 (q, 147)	174.2	205.5	88.8		−9.3
2c	$^{(1)}\ ^{(3)}\ ^{(2)}$ $HC-CO_2CH_3$ ‖ $HC-CO_2CH_3$	Ru	38.7 (d, 157)		51.9 (q, 146)	173.4	190.4, 193.7, 194.6[g]	91.2		−7.9
		Fe	46.6 (d, 161)		52.0 (q, 147)	172.5	206.6	83.5		−7.0

[a] Recorded on Bruker WH 270 instrument, in toluene-d_8, at ambient temperature unless noted otherwise. [b] Ppm downfield from Me_4Si, multiplicity and $^1J_{CH}$ (Hz) in parentheses. [c] $\Delta\delta = \delta$(olefin) − δ(complex). [d] At −45 °C. [e] At −50 °C. [f] At 0 °C. [g] The relative intensities of these resonances, in order of increasing downfield shift, are 1:1:2.

intensity. The force field parameters (Table II) are similar to those observed for the analogous iron complex,[11] with the exception of k_a which is significantly higher for ruthenium, thus indicating reduced M → CO π back-bonding. For the complexes **2a** and **2c** the assignment of the bands associated with the asymmetric CO stretching vibrations is less straightforward, due to their almost equal intensities. We have chosen the same assignment as for **2b** since the reverse ordering of the B_1 and B_2 modes results in negative i_e values. Reduced M → CO π back-bonding in the order **2a** > **2c** ≳ **2b** is manifested in the k parameters and reflects the increasing π acidity of the olefinic ligands.

We note the occurrence of two well-separated bands in the ν(CO ester) region of **2c** (Figure 1, Table I). We have found that the extra band does not arise from contamination of the complex with free dimethyl maleate. Upon reexamination a similar phenomenon is observed in the infrared spectrum of (η^2-dimethyl maleate)-Fe(CO)$_4$.[12] This must be due to different environments of the ester groups within one molecule or/and in different species. The corresponding fumarate complexes also exhibit two ester carbonyl bands, although with intensity ratios distinctly different from unity. This, in addition to several well discernible shoulders on the metal carbonyl bands of **2b** and **2c**, reveals that most probably more than one species is involved. We envisage different rotamers with the α,β-unsaturated ester moieties in coplanar (S cis and/or S trans) or perpendicular arrangements to be responsible for this phenomenon. In fact, a recent X-ray structure determination of tricarbonyl(η^2-diethyl maleate)(triphenylphosphine)iron[13] showed one ester group in a S cis-coplanar and the other one in a perpendicular orientation with respect to the olefinic double bond.

The ^1H NMR spectra of the complexes **2a–2c** show the expected upfield coordination shifts of the olefinic protons. These shifts are slightly larger than those in the analogous iron complexes (see Experimental Section).

The ^{13}C NMR spectroscopic data are presented in Table III. Carbonyl scrambling requires higher temperatures than in the case of the tetracarbonyliron derivatives. Hence, it is evident that, as has been shown previously,[6] the activation barrier for the coupled olefin rotation–Berry pseudorotation rearrangement is higher for the ruthenium compounds. Since the barrier for this process is mainly governed by the π component of the metal–olefin bond,[6,14,15] the higher activation barrier is consistent with an increase in the metal → π^*(olefin) back-bonding. However, this is apparently more than offset by a concomitant decrease in the π(olefin) → metal donor interaction since the ruthenium compounds are less stable than their iron analogues. In spite of this overall weakening of the metal–olefin bond, the olefin carbon atoms experience ~8–10 ppm larger upfield coordination shifts in the ruthenium complexes. This demonstrates that the coordination shifts originate predominantly in the π back-bonding component of the olefin–metal bond.[16-18]

Table IV. Disappearance Quantum Yields, ϕ_{-1}, for the Conversion $Ru_3(CO)_{12}$ (1) + olefin $\xrightarrow{h\nu}$ 3(η^2-olefin)Ru(CO)$_4$ (2)

olefin	dimethyl fumarate		methyl acrylate		
α[a]	5	25	5	25	2000
313 nm	0.009	0.043	0.023	0.039	0.121
395 nm	≲0.003	0.022	0.012	0.022	0.038

[a] Olefin/Ru ratio (number of olefin molecules present per Ru atom).

The chemical shifts of the carbonyl carbon atoms in (η^2-olefin)M(CO)$_4$ complexes of iron and ruthenium can also be accounted for in terms of π back-bonding arguments. In particular, for the latter compounds we observe higher CO stretching frequencies (Table I) and force constants (Table II), i.e., less back-donation, while the ^{13}C carbonyl resonances appear at higher field (Table III). Within each of the two series, the better π-accepting olefin (fumarate ≳ maleate > acrylate) leaves the metal with a reduced electron density available for the metal → π^*(CO) back donation, resulting in a slightly higher field carbonyl ^{13}C resonance (cf. ref 19), Upfield shifts of ^{13}C carbonyl resonances which parallel a decrease in metal → π^*(CO) back-donation have been observed before,[20] although the general applicability of such a correlation has been questioned.[21] We also note that increased shielding of the carbonyl carbon atoms in transition-metal complexes upon proceeding down a group appears to be a general phenomenon.[20] Surprisingly, the ester carbonyl ^{13}C resonances experience a downfield coordination shift similar to those described for the carbonyl ligands.

Electronic Spectra. In contrast to the yellow iron compounds[22] the (η^2-olefin)Ru(CO)$_4$ complexes are virtually colorless. This may be due to the stronger metal → π^*(olefin) interaction which stabilizes the highest occupied metal d_{xy} (b_2) orbital and thus gives rise to a blue shift of the MC (metal-centered) and MLCT transitions involving this orbital. The absorption curve shows no significant features but increases almost monotonously from ~380

(12) Koerner von Gustorf, E.; Henry, M. C.; McAdoo, D. J. *Justus Liebigs Ann. Chem.* **1967**, *707*, 190.
(13) Stainer, M. V. R.; Gittawong, S.; Takats, J., to be submitted for publication.
(14) Kruczynski, L.; LiShingMan, L. K. K.; Takats, J. *J. Am. Chem. Soc.* **1974**, *96*, 4006.
(15) Wilson, S. T.; Coville, N. J.; Shapley, J. R.; Osborn, J. A. *J. Am. Chem. Soc.* **1974**, *96*, 4038.
(16) Tolman, C. A.; English, A. D.; Manzer, L. E. *Inorg. Chem.* **1975**, *14*, 235.
(17) Salomon, R. G.; Kochi, J. K. *J. Organomet. Chem.* **1974**, *64*, 135.
(18) Thoennes, D. J.; Wilkins, C. L.; Trahanovsky, W. S. *J. Magn. Reson.* **1974**, *13*, 18.
(19) Von Büren, M.; Cosandey, M.; Hansen, H.-J. *Helv. Chim. Acta* **1980**, *63*, 738.
(20) Todd, L. J.; Wilkinson, J. R. *J. Organomet. Chem.* **1974**, *77*, 1.
(21) Evans, J.; Norton, J. R. *Inorg. Chem.* **1974**, *13*, 3042.
(22) Grevels, F.-W.; Koerner von Gustorf, E. *Justus Liebigs Ann. Chem.* **1975**, 547.

Scheme II

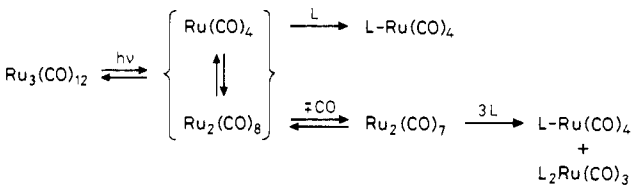

nm to a shoulder (**2b**, **2c**) or maximum (**2a**) at 250–270 nm; some data are given in the Experimental Section.

Quantum Yields, $\phi_{-Ru_3(CO)_{12}}$, and Mechanistic Aspects of (η^2-Olefin)Ru(CO)$_4$ Formation. The electronic absorption spectrum of $Ru_3(CO)_{12}$[23] exhibits a distinct maximum at 390 nm and two absorptions at 320 and 270 nm which appear as shoulders on an intense MLCT band (238 nm). In spite of some uncertainty concerning the precise ordering of the highest occupied molecular orbitals,[24,25] the longer wavelength absorptions should be associated with transitions which terminate in a σ^* orbital possessing antibonding character with respect to the Ru_3 framework.[23] In particular, the 390- and 320-nm absorptions have been assigned to $\sigma \rightarrow \sigma^*$ and $\sigma^{*\prime} \rightarrow \sigma^*$ transitions, respectively.[23] Hence, it is likely that such electronic excitations result in Ru–Ru bond cleavage and, in the presence of appropriate ligands, lead to the formation of mononuclear complexes.

We have determined the quantum yields, ϕ_{-1}, for reaction 1 with methyl acrylate and dimethyl fumarate as the olefinic substrates at two different wavelengths, 395 and 313 nm. The results are presented in Table IV. As mentioned before, the products **2a** and **2b** are stable under the reaction conditions, and no other products were observed, even at 313 nm and up to 40% conversion of **1**. The quantum yields improve considerably with increasing olefin concentration. This can be interpreted in terms of the formation of an intermediate which either reforms $Ru_3(CO)_{12}$ or is competitively trapped by the olefin. For methyl acrylate ϕ_{-1} seems too approach limiting values of ~0.12 at 313 nm and ~0.04 at 395 nm, respectively, at high olefin concentrations. This could not be verified for the dimethyl fumarate case due to the lower solubility of this olefin. As indicated by the ϕ_{-1} values at low olefin concentrations, methyl acrylate seems to be more effective than the bulkier dimethyl fumarate in trapping the intermediate.

There has been some speculation about the primary photocleavage reaction of the $Ru_3(CO)_{12}$ cluster. An open-chain diradical species has been proposed[5] which could undergo either reclosure or subsequent thermal reactions with an appropriate substrate. Extrusion of $Ru(CO)_4$, directly from the parent cluster or subsequently to step 2, may be considered as a reasonable

$$Ru_3(CO)_{12} \overset{h\nu}{\rightleftharpoons} \cdot Ru(CO)_4\text{–}Ru(CO)_4\text{–}Ru(CO)_4\cdot \rightarrow \quad (2)$$

mechanistic feature. The binuclear species $Ru_2(CO)_8$ left behind could react further according to Scheme II, which could account for the simultaneous formation of L–Ru(CO)$_4$ and $L_2Ru(CO)_3$ (L = $P(C_6H_5)_3$,[3,4,26] L = $P(OCH_3)_3$[8]) under conditions where L–Ru(CO)$_4$ does not absorb light.[4,8] The analogous iron species, $Fe_2(CO)_8$, has been observed under low-temperature matrix isolation conditions[27] and was proposed to be formed in solution by dimerization of $Fe(CO)_4$.[28] It is not clear, however, why $L_2Ru(CO)_3$ is formed as a primary photoproduct with *n* donor ligands but not with olefins.

Whatever the actual reaction pathway in the formation of L–Ru(CO)$_4$ complexes may be, there is little doubt that at 395 nm the initial step involves Ru–Ru bond cleavage. This may not necessarily hold true for the photolysis at 313 nm. It has been pointed out, with regard to the photochemical behavior of $Os_3(CO)_{12}$,[29] that the $\sigma^{*\prime} \rightarrow \sigma^*$ excited state has a partial M–CO antibonding character. Accordingly, initial loss of CO with formation of $Ru_3(CO)_{11}L$ and subsequent decay of the cluster seems possible and has been proposed to be operative in part in the photochemical reaction of $Ru_3(CO)_{12}$ with phosphines.[3,26] Flash photolysis experiments with $Ru_3(CO)_{12}$[30] provide evidence for the formation of two distinct transients both of which appear to be primary photoproducts. One of the two species seems to arise from the parent cluster by loss of CO, the other one could be the open-chain diradical. In view of these aspects we considered a study of the effect of CO on the quantum yield of the conversion of $Ru_3(CO)_{12}$ into (η^2-olefin)Ru(CO)$_4$. However, as has been pointed out before, under CO atmosphere the formation of $Ru(CO)_5$ interferes with the reaction to be studied, thus seriously impeding the quantum yield measurements.

It must be emphasized that photoreactions of $Ru_3(CO)_{12}$ at wavelengths $\lesssim$320 nm could originate, at least in part, in a CT excited state, since the events in the spectrum at 320 and 270 nm are merely shoulders on the strong MLCT band centered at 238 nm.[23] In any case, from the higher quantum yields observed at 313 nm we have to conclude that direct reaction from one of the higher excited states contributes significantly to the product formation; i.e., complete internal conversion to (and exclusive reaction via) the lowest $\sigma \rightarrow \sigma^*$ excited state can be ruled out.

Experimental Section

All reactions and manipulations were carried out under argon and in argon-saturated solvents. Irradiations were performed in an immersion lamp apparatus using a high pressure mercury lamp Philips HPK 125 W surrounded by a GWV (Glaswerk Wertheim) cutoff filter tube ($\lambda \gtrsim$ 370 nm). Spectra were recorded by using the following instruments: NMR, Bruker WH 270; IR, Perkin-Elmer 580 (calibrated with DCl[31]) and 257; UV–visible, Perkin-Elmer 554 and Cary 219; mass spectra, Varian MAT CH5. Melting points were determined on a Reichert Kofler apparatus. Microanalyses were performed by Dornis & Kolbe, Mülheim a.d. Ruhr. Analytical grade solvents (Merck) were used as received. $Ru_3(CO)_{12}$ was purchased from Strem Chemicals Inc.; the other chemicals were Merck synthetic grade reagents which were recrystallized or distilled in vacuo before use.

Preparation of (η^2-Olefin)Ru(CO)$_4$. General Procedure. $Ru_3(CO)_{12}$ is added to a degassed solution of the selected olefin in 200 mL of hexane. If gram quantities of $Ru_3(CO)_{12}$ are used, a slurry is obtained initially. As the reaction proceeds, upon irradiation, the solid $Ru_3(CO)_{12}$ gradually dissolves. Irradiation, at 10–15 °C, is continued until the orange-yellow color of $Ru_3(CO)_{12}$ had disappeared (3–6 h). The reaction can also be monitored conveniently by means of infrared spectroscopy which shows the exclusive formation of (η^2-olefin)Ru(CO)$_4$. The solution is filtered, if necessary, and concentrated to about half the original volume by evaporating the solvent in vacuo at 0 °C or below. Upon cooling of the mixture to −78 °C the complexes **2** precipitate as white crystals within 2–3 days. The supernatant solution is removed and the crystals dried in vacuo at 0 °C or below. The complexes are recrystallized from hexane to which free olefin is added.

2a. A 1.92-g sample of $Ru_3(CO)_{12}$ (3 mmol) and 7.5 g of methyl acrylate (91.5 mmol) gave 2.23 g of **2a** (83%). During the workup procedure the temperature was kept at $\lesssim$−30 °C; **2a** starts to decompose above −10 °C. Anal. Calcd for $C_8H_6O_6Ru$: C, 32.11; H, 2.02. Found:

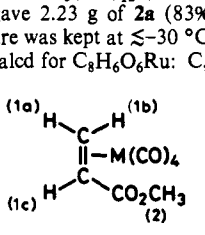

C, 32.16; H, 1.88. ^{1}H NMR data (in parentheses the data for the

(23) Tyler, D. R.; Levenson, R. A.; Gray, H. B. *J. Am. Chem. Soc.* **1978**, *100*, 7888.
(24) Green, J. C.; Seddon, E. A.; Mingos, D. M. P. *J. Chem. Soc., Chem. Commun.* **1979**, 94.
(25) Ajó, D.; Granozzi, G.; Tondello, E.; Fragalá, I. *Inorg. Chim. Acta* **1979**, *37*, 191.
(26) Johnson, B. F. G.; Lewis, J.; Twigg, M. V. *J. Chem. Soc., Dalton Trans.* **1975**, 1876.
(27) Poliakoff, M.; Turner, J. J. *J. Chem. Soc. A* **1971**, 2403; *J. Chem. Soc., Dalton Trans.* **1974**, 2276.
(28) Fischler, I.; Hildenbrand, K.; Koerner von Gustorf, E. *Angew. Chem.* **1975**, *87*, 35; *Angew. Chem., Int. Ed. Engl.* **1975**, *14*, 54.
(29) Tyler, D. R.; Altobelli, M.; Gray, H. B. *J. Am. Chem. Soc.* **1980**, *102*, 3022.
(30) Meyer, T. J., private communication to J.T., August 1980.
(31) "Tables of Wavenumbers for the Calibration of Infrared Spectrometers"; compiled by Cole, A. R. H.; Pergamon Press: Oxford, 1977; p 134–137.

analogous iron complex and the free olefin): δ 1.74, H^{1a} (2.20, 5.35); 2.47, H^{1b} (2.75, 6.35); 2.81, H^{1c} (3.08, 5.95); 3.29, H^2 (3.41, 3.49); J_{gem} = 3.0 Hz, J_{cis} = 8.1 Hz, J_{trans} = 11.1 Hz; in toluene-d_8 at -40 °C (and ambient temperature, respectively). UV-visible data: 268 nm (max, ε ≈ 7000), in hexane which contains 0.5% methyl acrylate; the same solution was used in the reference cell.

2b. A 0.19-g sample of $Ru_3(CO)_{12}$ (0.3 mmol) and 0.13 g of dimethyl fumarate (0.9 mmol) gave 0.19 g of **2b** (59%), mp 101-102 °C. Anal. Calcd for $C_{10}H_8O_8Ru$: C, 33.61; H, 2.26; Ru, 28.29. Found: C, 33.40; H, 2.08; Ru, 28.48. The mass spectrum shows prominent peaks (^{102}Ru containing fragments) at *m/e* 330, 302, 274, and 246 ($M^+ - nCO$, *n* = 1-4), 327 ($M^+ - OCH_3$) and further fragmentation products at *m/e* 216, 188, 158, 130, and 102. ^1H NMR data: δ 3.73, H^1 (3.83, 6.86); 3.33, H^2 (3.35, 3.31); in benzene-d_6 at ambient temperature. UV-visible data: ~295 (wsh, ε = 4350), ~250 (sh, ε = 9100), 227 nm (ε = 9950).

2c. A 0.19-g sample of $Ru_3(CO)_{12}$ (0.3 mmol) and 0.13 g of dimethyl maleate (0.9 mmol) gave 0.29 g of **2c** (90%), mp 45-45.5 °C. Anal. Calcd for $C_{10}H_8O_8Ru$: C, 33.61; H, 2.26; Ru, 28.29. Found: C, 33.98; H, 2.06; Ru, 27.98. The mass spectrum is similar to that of **2b**. ^1H NMR data: δ 3.05, H^1 (3.09, 5.96); 3.48, H^2 (3.41, 3.46); in benzene-d_6 at ambient temperature. UV-visible data: ~250 (wsh, ε = 7150), 226 nm (ε = 9150).

2d and **2f** have been isolated by a similar procedure as white solids; however, due to the instability of these compounds yields could not be accurately determined, and physical data other than CO stretching frequencies (Table I) are still lacking.

Quantum Yield Determinations. Quantum yields (reproducible within ±5%) were determined by using an electronically integrating actinometer which was calibrated by ferrioxalate actinometry.[32] The actinometer has been described elsewhere[33] and compensates for incomplete absorption of light in the sample cell. All experiments were carried out at 298 ± 1 K in degassed hexane solutions containing ~2.2×10^{-4} M $Ru_3(CO)_{12}$. Irradiations at 313 or 395 nm were performed in quartz cuvettes (*d* = 1 cm), using a Hanovia 1000 W Hg-Xe lamp in connection with a Schoeffel Instruments GM 250 single-grating monochromator. Light intensities were in the order of 10^{-6}-10^{-5} E min^{-1}. Disappearance of $Ru_3(CO)_{12}$ was monitored by measuring the absorption at the 390-nm maximum. Constant ϕ_{-1} values were obtained at both wavelengths, 313 and 395 nm, over a wide range of conversion (up to 40%). At 313 nm appropriate corrections were made in order to account for internal light filter effects due to the tail absorptions of **2a** and **2b**. The following ε values (1 mol^{-1} cm^{-1}) were used: ε[$Ru_3(CO)_{12}$] = 7360 at 390 nm (values reported in the literature are 7700[4] and 6400[23]) and 9300 at 313 nm; ε (**2a**) = 2240 and ε (**2b**) = 2380 at 313 nm.

Acknowledgment. We wish to thank the staff of the spectroscopic laboratories for their help and Herrn K. Schneider for experimental assistance. J.T. is indebted to the Alexander von Humboldt Foundation for support of this research by a fellowship during his stay at the Institut für Strahlenchemie in 1978/1979.

(32) Hatchard, C. G.; Parker, C. A. *Proc. R. Soc. London, Ser. A* **1956**, *235*, 518. Murov, S. L. in "Handbook of Photochemistry"; Marcel Dekker: New York, 1976; p 119.
(33) Amrein, W.; Gloor, J.; Schaffner, K. *Chimia* **1974**, *28*, 185.

The Synthesis, Redox Properties, and Ligand Binding of Heterobinuclear Transition-Metal Macrocyclic Ligand Complexes. Measurement of an Apparent Delocalization Energy in a Mixed-Valent Cu^ICu^{II} Complex

R. R. Gagné,*[1] C. L. Spiro,[1] T. J. Smith,[2] C. A. Hamann,[1] W. R. Thies,[2] and A. K. Shiemke[2]

Contribution No. 6276 from the Division of Chemistry and Chemical Engineering, California Institute of Technology, Pasadena, California 91125. *Received August 4, 1980*

Abstract: A series of binuclear complexes $M_A^{II}M_B^{II}L^{2+}$ have been synthesized and characterized. The binucleating macrocyclic ligand L^{2-} is a symmetric Schiff base derived by condensing 2 equiv of 2,6-diformyl-4-methylphenol with 2 equiv of 1,3-diaminopropane, resulting in two identical N_2O_2 coordination sites. In all cases, $M_A(II)$ = Cu(II) while M_B was varied across the series $M_B(II)$ = Mn(II), Fe(II), Co(II), Ni(II), Cu(II), and Zn(II). The electrochemical properties of these species were examined by cyclic voltammetry, differential pulse polarography, sampled DC polarography, and coulometry. In each case reversible to quasi-reversible Cu(II)Cu(I) electrochemistry was observed. The Cu(II)Cu(I) reduction potential was, within experimental error, invariant with respect to the remote metal M_B; E_f(Cu(II)Cu(I)) = -1.068 V vs. ferrocene/ferrocinium(1+). The one exception is the homobinuclear complex $M_A(II) = M_B(II)$ = Cu(II); the homobinuclear complex was more readily reduced, E^f = -0.925 V vs. Fc/Fc^+, than the heteronuclear species. After a correction due to magnetic stabilization the difference between the heteronuclear and homonuclear reduction potentials, 143 mV = 3.3 kcal/mol, has been ascribed to a special stability associated with the mixed-valent $Cu^{II}Cu^IL^+$ species, where some electronic delocalization has been previously demonstrated. In addition, the electrochemical properties of homonuclear complexes ($M_A = M_B$) are reported. The ligand-binding properties of the species $Cu^IM_B^{II}L^+$, $M_B(II)$ = Mn(II), Fe(II), Co(II), Ni(II), Cu(II), and Zn(II), have been examined. Cu(I) shows an affinity for the axial bases carbon monoxide, ethylene, tris(*o*-methoxyphenyl)phosphine, and 4-ethylpyridine. In contrast to the Cu(II)/Cu(I) reduction potentials, the binding of axial bases to Cu(I) does seem to depend on the nature of the remote metal, M_B.

Multimetallic species occupy an important position in modern inorganic chemistry. They are ubiquitous in nature as active sites in a variety of metalloenzymes and are playing a significant and expanding role in industrial chemical catalysis.

The importance of multimetallic species has prompted a wide range of theoretical treatments concerning their properties. These include orbital models for magnetic exchange coupling,[3] potential energy surface treatments of thermal intramolecular electron

(1) California Institute of Technology.
(2) Kalamazoo College, Kalamazoo, Mich.

(3) P. J. Hay, J. C. Thibeault, and R. Hoffmann, *J. Am. Chem. Soc.*, **97**, 4884 (1975).

0002-7863/81/1503-4073$01.25/0